JOURNAL OF VIROLOGY, July 2008, p. 6272–6287 Vol. 82, No. 13
0022-538X/08/$08.00+0 doi:10.1128/JVI.02345-07

Multimerization of Tegument Protein pp28 within the Assembly Compartment Is Required for Cytoplasmic Envelopment of Human Cytomegalovirus▽

Jun-Young Seo[1] and William J. Britt[1,2,3]*

Departments of Microbiology,[1] Pediatrics,[2] and Neurobiology,[3] School of Medicine, University of Alabama in Birmingham, Birmingham, Alabama 35233

Received 30 October 2007/Accepted 25 March 2008

Human cytomegalovirus (HCMV) UL99-encoded pp28 is an essential tegument protein required for envelopment and production of infectious virus. Nonenveloped virions accumulate in the cytoplasm of cells infected with recombinant viruses with the UL99 gene deleted. Previous results have suggested that a key function of pp28 in the envelopment of infectious HCMV is expressed after the protein localizes in the assembly compartment (AC). In this study, we investigated the potential role of pp28 multimerization in the envelopment of the infectious virion. Our results indicated that pp28 multimerized during viral infection and that interacting domains responsible for self-interaction were localized in the amino terminus of the protein (amino acids [aa] 1 to 43). The results from transient-expression and/or infection assays indicated that the self-interaction took place in the AC. A mutant pp28 molecule containing only the first 35 aa failed to accumulate in the AC, did not interact with pp28 in the AC, and could not support virus replication. In contrast, the first 50 aa of pp28 was sufficient for the self-interaction within the AC and the assembly of infectious virus. Recombinant viruses encoding an in-frame deletion of aa 26 to 33 of pp28 were replication competent, whereas infectious virus was not recovered from HCMV BACs lacking aa 26 to 43. These findings suggested that the accumulation of pp28 was a prerequisite for multimerization of pp28 within the AC and that pp28 multimerization in the AC represented an essential step in the envelopment and production of infectious virions.

Human cytomegalovirus (HCMV) is an important human pathogen associated with acute and chronic disease in both normal and immunocompromised populations (4, 34, 45, 46). The virus is the largest and most complex member of the family of human herpesviruses. The virion of HCMV consists of three distinct structures: a nucleocapsid containing a 230-kbp linear DNA genome that may encode over 200 open reading frames (ORFs), an envelope including an as-yet-undefined number of viral glycoproteins, and a tegument layer located between the capsid and envelope (31, 32, 49, 53, 55). In addition, the virion contains a minimum of 71 virus-encoded proteins and a large number of host-derived proteins (50).

HCMV assembly is a multistage, poorly understood process. Although all proposed models include well-studied mechanisms of capsid assembly within the nucleus of infected cells, the final tegumentation and envelopment in the cytoplasm of infected cells remains poorly understood (29). Early ultrastructural studies of herpes simplex virus (HSV) and HCMV noted that nonenveloped cytoplasmic particles in HCMV-infected cells were coated with a thick tegument layer but that nonenveloped HSV particles often had the appearance of naked capsids (44). These and other findings suggested that, in contrast to the assembly of HSV and other alphaherpesviruses, tegument proteins could play a key role in the cytoplasmic phase of HCMV assembly and that the cytoplasmic assembly of HSV and HCMV could differ substantially.

Recently, several laboratories have approached the investigation of the cytoplasmic tegumentation of HCMV by studying the role of a tegument protein, pp28, in virus assembly. This protein contains 190 amino acids (aa) encoded by the UL99 ORF (10). It is a true late protein that is myristoylated and phosphorylated (22, 24, 37, 42). In addition, preliminary findings have suggested that pp28 is also palmitoylated and possibly ubiquitinated (J.-Y. Seo, unpublished data). The pp28 protein is one of the most abundant constituents of the tegument layer (6, 30, 50). In studies of virus assembly this protein is essential for the production of infectious virus and deletion of the UL99 ORF resulted in the production of nonenveloped and noninfectious cytoplasmic particles (3, 22, 42). The pp28 protein is localized to the endoplasmic reticulum-Golgi intermediate compartment (ERGIC) in the absence of other viral proteins (37). In virus-infected cells it is localized to a cytoplasmic compartment designated the virus assembly compartment (AC) late in infection, and viral functions are required for its localization to the AC (36, 37). The AC is thought to be a modified compartment of the cellular secretory system and possibly derived from late endosomes (36, 40, 48). Localization of pp28 to the AC is required for virus assembly, and mutations that impair its localization in the AC also limit the production of infectious virus (40). Two previous studies have shown that the first 60 aa of pp28 alone are sufficient for the generation of viruses exhibiting an assembly and replication phenotype that is indistinguishable from wild-type virus (22, 40). In addition, these same studies demonstrated that deletion of an acidic amino acid cluster (aa 44 to 59) of pp28 led to the loss of the

* Corresponding author. Mailing address: Department of, Pediatrics, Room 107, Harbor Bldg., Children's Hospital, 1600 7th Ave. South, Birmingham, AL 35233. Phone: (205) 996-7762. Fax: (205) 975-6549. E-mail: wbritt@peds.uab.edu.

▽ Published ahead of print on 2 April 2008.

recovery of infectious virus, suggesting that this stretch of amino acids is essential for the assembly of infectious virions (22, 40). The precise role of this acidic cluster in the function of pp28 in the assembly of infectious HCMV remains unknown. We previously characterized a replication-impaired virus mutant encoding only the first 50 aa (containing a half of the acidic amino acid cluster) of pp28 (40). Our data indicated that the mutant pp28 protein encoded by this virus appeared to contribute to a loss of envelopment secondary to its delayed accumulation in the AC of infected cells, arguing that the role of pp28 in envelopment is expressed after its localization in the AC (40). Previous studies have demonstrated higher-molecular-weight forms of pp28 in sodium dodecyl sulfate-polyacrylamide gel electrophoresis (SDS-PAGE) and Western blot analysis, suggesting that this protein multimerizes in the infected cell, raising the possibility that multimerization represented a postlocalization function of pp28 essential for virion assembly.

A significant number of reports have shown that multimerization of tegument or matrix proteins (MAs) in structurally less complex viruses, such as small RNA viruses, play an essential role in the viral assembly. Multimerization of viral MAs has been proposed to lead to the formation of a protein lattice that can lead to membrane deformation and eventual budding through that region of the membrane (11, 18, 21, 23, 39). Although several studies have demonstrated the critical role of pp28 in envelopment of the infectious particle, it is unknown whether specific postlocalization functions of pp28, possibly multimerization, and/or interactions with other viral or cellular proteins in the AC contribute to the envelopment process.

In the present study, we investigated the role of pp28 multimerization in the envelopment of infectious HCMV. Initially, we confirmed that multimers of pp28 were present in infected cells. In virus-infected cells, pp28 multimerized with definable kinetics, suggesting that higher-molecular-weight forms of pp28 were indeed multimers and not protein aggregates. Utilizing bacterially derived pp28 and pp28 mutants in pulldown assays we could demonstrate pp28 self-interactions. Domains of pp28 required for self-interactions were mapped to the amino terminus of the molecule. These results were confirmed by using fluorescence resonance energy transfer (FRET) assays. Additional studies using both FRET assays and subcellular fractionation of infected cell proteins by sedimentation through density gradients indicated that pp28 multimerization appeared to occur in the AC in virus-infected cells. These result also suggested that the interacting domain for multimerization is distinct from a trafficking signal for authentic localization to the AC. Finally, the findings of the present study indicated that pp28 multimerizes through self-interaction within the AC during viral infection and that pp28 multimerization within the AC was a postlocalization function required for the assembly and envelopment of infectious virus.

MATERIALS AND METHODS

Cells, viruses, and antibodies. Primary human foreskin fibroblasts (HFFs) were prepared, propagated, and infected as previously described (5, 8). HCMV strain AD169 was used for all experiments. An infectious stock was prepared from supernatants of infected HFF cells that exhibited a 100% cytopathic effect, and titers were determined as described previously (5, 8). COS-7 and HK293 cells were maintained in Dulbecco modified Eagle medium (DMEM) supplemented with 5% newborn calf serum and penicillin-streptomycin. The antibodies used in the present study include anti-pp28; monoclonal antibody (MAb) 41-18; anti-pp65 (BB epitope); MAb 28-19; anti-IE1 (UL123); MAb P63-27 (36); and anti-enhanced green fluorescent protein (anti-EGFP), a rabbit antiserum (Invitrogen, Carlsbad, CA).

SDS-PAGE and immunoblotting. SDS-PAGE under reducing and nonreducing conditions was carried out as described previously (1, 12). The resolving and stacking gels contained 0.1% SDS. Under denaturing conditions, samples were solubilized in sample buffer containing 2% SDS and 5% 2-mercaptoethanol and then heated to 100°C. For conditions described as less denaturing and nonreducing conditions, samples were solubilized in sample buffer containing 0.1% or 2% SDS without heating. The solubilized proteins were then subjected to SDS-PAGE and transferred onto nitrocellulose membranes. Samples were analyzed by Western blotting as described in previous publications and developed using enhanced chemiluminesence (Pierce Biotechnology, Rockford, IL).

[^{35}S]Met-Cys labeling and sedimentation analysis of pp28 multimerization. HCMV-infected HFF cells or HK293 cells transfected with an expression plasmid encoding pp28 were radiolabeled with 100 μCi of [^{35}S]methionine-cysteine ([^{35}S]Met-Cys) per ml as previously described (1, 7, 8). After solubilization in standard radioimmunoprecipitation assay buffer (0.1% NP-40, 1% deoxycholate, and 0.1% SDS in Tris-buffered saline [TBS; 50 mM Tris, 150 mM NaCl; pH 7.5]), the labeled proteins were precipitated with MAbs, and the precipitated proteins were analyzed by SDS-PAGE as described in previous publications (1, 7, 8). The assay for multimerization has been described in detail in an earlier publication (7, 8). Briefly, monolayers of HCMV-infected HFF cells or HK293 cells transfected with an expression plasmid were washed and Met-Cys starved for 60 min. The cells were then incubated in Met-Cys-free medium containing 100 μCi of [^{35}S]Met-Cys (New England Nuclear, Boston, MA) per ml for 10 min and then, after extensive washing, the cells were either harvested by placing the dishes at −80°C or chased with medium containing Met and Cys and supplemented with 100 μg of cycloheximide per ml for 20 and 40 min. These cultures were harvested and placed at −80°C. The labeled monolayers were solubilized in TBS containing 0.1% NP-40 at 4°C for 30 min, and solubilized proteins were precleared by incubation with normal goat serum and staphylococcal Cowan I bacteria (Calbiochem, San Diego, CA), followed by centrifugation for 15 min at 13,000 × *g*. The cleared lysate was applied to preformed 5 to 40% linear sucrose gradients and centrifuged for 20 h at 34,000 rpm in a Beckman SW41 rotor. The gradients were fractionated from the bottom into 1-ml fractions, and each fraction was precipitated with the specified antibody. The immune precipitates were collected by first adding rabbit anti-mouse immunoglobulin G (IgG; Cappel Laboratories, Aurora, OH), followed by staphylococcal Cowan I bacteria. After extensive washing, the immune precipitates were analyzed by SDS-PAGE in 10% gels. Migration of the radiolabeled protein down the gradient, as reflected by recovery of the radiolabeled protein in fractions more proximal to the bottom of the gradient, indicated multimerization of the protein.

GST-pulldown assay. A series of glutathione *S*-transferase (GST)–pp28 fusion proteins in which GST was fused with pp28 wild type; pp28 mutants expressing the first 33, 61, 90, and 123 aa of pp28; and three deletion mutants in which aa 26 to 33, aa 26 to 43, or aa 44 to 59, an acidic domain was deleted, and a BB epitope (RKTPRVTG fused to NH_2 terminus)-tagged wild-type pp28 (BB-pp28) protein were expressed and induced in *Escherichia coli* (BL21). Bacterial lysates containing recombinant proteins from a 30-ml culture were prepared by using Bugbuster protein extraction reagent (BPE reagent; Novagen, La Jolla, CA) according to the manufacturer's instructions. Briefly, bacterial cell pellets were resuspended in 1 ml of BPE reagent, followed by incubation for 15 min at room temperature. The solubilized lysates were pelleted at 1,600 × *g* for 20 min at 4°C. The lysate supernatants were used in the pulldowns. All binding steps were performed in a 1-ml reaction volume with BPE reagent. A total of 30 μl of a 50% (vol/vol) slurry of glutathione-Sepharose beads (Amersham Biosciences, Piscataway, NJ), prepared as described previously (9, 26), was added to each reaction mixture as described below. The supernatants of bacterial lysates containing equivalent amounts of GST fusion protein (as normalized by staining polyacrylamide gels with Coomassie blue) were adsorbed to glutathione-Sepharose beads for 1 h at room temperature. The beads were washed three times with BPE reagent and pelleted by centrifugation at 1,000 × *g* for 5 min in a microcentrifuge. The supernatants of bacterial lysates containing BB-pp28 were precleared with glutathione-Sepharose beads for 2 h at room temperature and then incubated with the purified GST proteins on glutathione-Sepharose beads for 1 h at room temperature. The beads were again pelleted and then washed with BPE reagent three times. The beads were resuspended in sample buffer containing 2% SDS and 5% 2-mercaptoethanol, heated to 100°C for 5 min, and pelleted. The supernatants were then subjected to SDS-PAGE in 10% gels. The gels were either stained with Coomassie blue or visualized by Western blotting with anti-

pp28 MAb 41-18 and anti-BB tag MAb 28-19, followed by the addition of horseradish peroxidase-conjugated goat anti-mouse IgGs secondary antibody and enhanced chemiluminescence. MAb 28-19 is reactive with peptide (RKTP RVTG) encoded by HCMV UL83.

Acceptor photobleaching FRET by confocal microscopy. For FRET assays, mutant and full-length pp28 proteins were coexpressed in Cos-7 cells after transfection of plasmids encoding the first 25, 30, 35, 50, or 61 aa of pp28 or the full-length pp28 molecule fused at the C terminus to EGFP and a plasmid encoding the full-length pp28 molecule tagged on the C terminus with monomeric red fluorescence protein (DsRed). The transfected Cos-7 cells were grown on a 13-mm glass coverslip at 37°C in DMEM containing 10% fetal calf serum. At day 2 posttransfection, the Cos-7 cells on a coverslip were washed with phosphate-buffered salt solution (pH 7.4; PBS) and fixed in 2% paraformaldehyde for 10 min. A drop of mounting medium (50% glycerol in PBS) was added, and the coverslip was mounted and sealed on slides. In addition, EGFP fused with DsRed (EGFP-DsRed) or Golgi-associated, gamma adaptin ear-containing, ARF-binding protein 1 fused with EGFP (GGA1-EGFP) was prepared as a positive or a negative control, respectively, in transfected Cos-7 cells. FRET was processed by using a donor dequenching and acceptor photobleaching protocol on a confocal laser scanning microscope (Leica SP2; Leica, Bannockburn, IL). An excitation wavelength of 488 nm and an emission range of 500 to 550 nm and an excitation wavelength of 561 nm and an emission range of 580 to 700 nm were used to acquire images of EGFP and DsRed, respectively. DsRed was photobleached by using full power of the 561-nm line on a 0.3 regular set. An image of EGFP fluorescence and DsRed fluorescence after photobleaching was obtained by using the respective filter sets. Such data were collected from 5 to 10 different cells in different fields from the same coverslip. One to three regions of interest (ROI) in the photobleached area were selected per cell, and the mean EGFP fluorescence before and after photobleaching was obtained by using Leica confocal software. FRET efficiency was calculated by using the following relationship: FRET efficiency (%) = $[(D_{post} - D_{pre})/D_{post}] \cdot 100$. Here, D_{post} is the fluorescence intensity of the EGFP (donor [D]) after photobleaching, and D_{pre} is the fluorescence intensity of the DsRed before photobleaching. A nonbleaching region was selected as an internal control on FRET analysis. The data sets were analyzed statistically for differences in mean FRET, and P values of <0.05 are indicated in the figures.

A similar experiment utilizing FRET was performed in transfected and/or infected cells. FRET analysis was performed at day 6 postinfection in HFF cells in which a DsRed-tagged pp28 protein was coexpressed after electroporation of a plasmid encoding the first 35, 50, or 61 aa of pp28 or the full-length pp28 molecule fused at the C terminus to EGFP. Electroporated HFF cells were infected with HCMV 48 h later at a multiplicity of infection (MOI) of 0.1. The infected HFF cells were grown on a 13-mm glass coverslip at 37°C in DMEM containing 10% fetal calf serum. At day 6 postinfection, the infected HFF cells on a coverslip were washed with PBS, fixed in 2% paraformaldehyde for 10 min, and then stained with anti-IE-1 MAb, followed by fluorescein isothiocyanate-labeled anti-mouse IgG to identify the infected cells. The coverslip was mounted in 50% glycerol-PBS and sealed on the slides. FRET was processed by using the donor dequenching/acceptor photobleaching protocol described above.

Subcellular fractionation. A 75-cm^2 flask of HFF cells was electroporated with 5 μg of an expression vector encoding pp28Mut35-EGFP or pp28Mut61-EGFP After 24 h, the cells were washed and infected with HCMV at an MOI of 0.1. The HFF cells were harvested on day 6 postinfection by trypsinization, and the cell pellet was washed twice with cold PBS and resuspended in 1 ml of homogenization buffer (0.25 M sucrose, 10 mM HEPES [pH 7.4], 1 mM EDTA). The cell suspension was repeatedly passed through a 23-gauge needle until there were no intact cells in the suspension, as determined by light microscopy, and a postnuclear supernatant (PNS) was collected after centrifugation at 1,000 × g for 10 min. Subcellular fractionation was performed by using a density gradient prepared from iodixanol (Optiprep; Sigma, St. Louis, MO), and ultracentrifugation was performed using a modification of protocols described previously (40, 43, 52). A discontinuous gradient was prepared using 30, 25, 20, 15, and 10% (vol/vol) Optiprep solutions. The gradient was allowed to equilibrate vertically for 30 min at room temperature. The PNS was overlaid onto the discontinuous gradient and centrifuged at 100,000 × g in an SW41 rotor for 3 h at 4°C. Equal fractions were collected from the top of the gradient, and individual fractions were assayed for pp28Mut35-EGFP, pp28Mut61-EGFP, viral pp28 proteins, and the cellular protein CD63 by immunoblotting.

Construction of recombinant viruses. Recombinant viruses were constructed by using recombineering, as has been described in earlier studies with modifications using a *galK* selection system (40, 51). Viruses were recovered after electroporation of BAC DNA into primary human fibroblasts as described above. Virus yield assays were carried out as previously described (40).

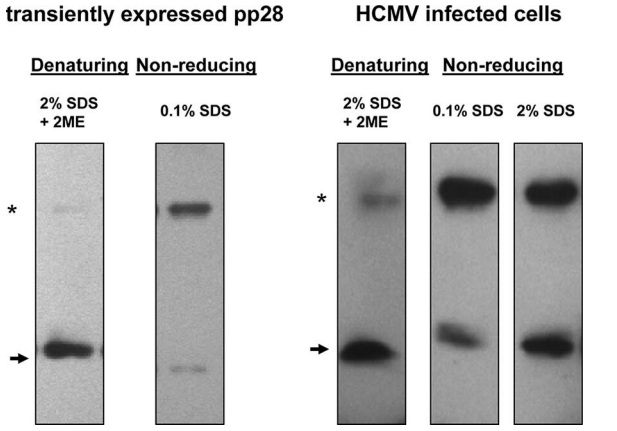

FIG. 1. Expression of multimeric forms of pp28. HK293 cells were transfected with a plasmid encoding pp28, harvested at day 2 posttransfection, and HFF cells were infected with HCMV (AD169) at an MOI of 0.1 and harvested at day 6 postinfection. In both cases, the cells were solubilized under denaturing (2% SDS and 5% 2-mercaptoethanol) and less denaturing and nonreducing (0.1 or 2% SDS) conditions, subjected to SDS-PAGE in 10% gel, and detected with anti-pp28 MAb by Western blot analysis as described in Materials and Methods. Arrows indicate the migration of monomeric pp28 based on its predicted amino acid sequence. Asterisks indicate the migration of what is presumed to be a multimeric form of wild-type pp28.

RESULTS

pp28 multimerizes during viral assembly. Previous studies from our laboratory and other laboratories have reported that additional higher-molecular-weight forms of pp28 could be observed in Western blot analysis of virus-infected cells, as well in cells transiently expressing pp28 in the absence of other viral proteins (Fig. 1) (22, 40). These findings raised that possibility that pp28 multimerized during virion assembly, perhaps through self-interactions. To determine whether higher-molecular-weight forms of pp28 were multimeric forms and not aggregated or misfolded forms of pp28, we carried out the experiments in which transiently expressed pp28 or viral pp28 was solubilized under denaturing (2% SDS and 5% 2-mercaptoethanol) and less denaturing and nonreducing (0.1% SDS or 2% SDS) conditions. Higher-molecular-weight forms of pp28 were detected when samples were disrupted in nonreducing conditions, suggesting that this form was a multimer of pp28. Moreover, it suggested that the predominant form of the pp28 molecule was a dimer (90%) rather than a monomer (10%) when analyzed in lower concentrations of SDS (0.1% SDS) under nonreducing conditions. In addition, the detection of higher-molecular-weight forms after SDS-PAGE in the absence of reducing agents suggested that the multimerization of pp28 could include the formation of intermolecular disulfide bonds.

Multimerization of pp28 in virus-infected cells was analyzed by density gradient centrifugation of infected cell proteins after pulse-chase radiolabeling. After cell lysis, labeled proteins were fractionated by centrifugation through sucrose density gradients, and each fraction was analyzed by immunoprecipitation and SDS-PAGE (2). In the later chase intervals, pp28 was detected in fractions of increasing sucrose density compared to pp28 synthesized during the pulse or in early chase intervals (Fig. 2A). The kinetics of the formation of the higher-

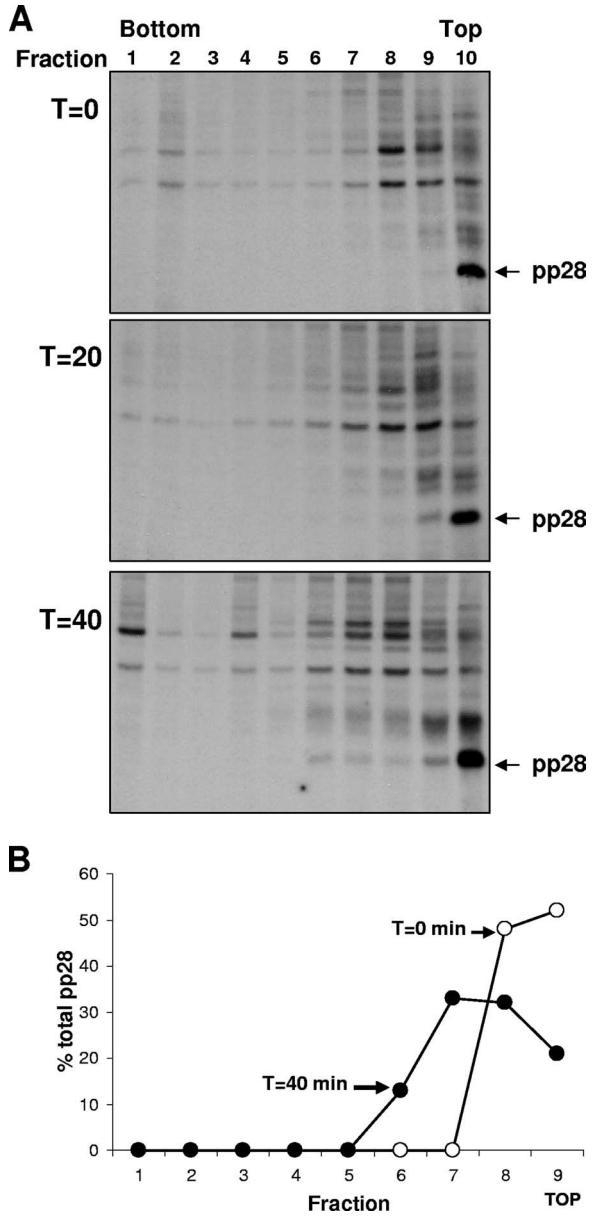

FIG. 2. Multimerization of pp28 through the self-interaction. (A) HFF cells were infected with HCMV (AD169) at an MOI of 0.1 and labeled with [^{35}S]Met-Cys and then chased in cycloheximide-containing medium for the indicated times as described in Materials and Methods. Cells were solubilized, loaded onto a 5 to 40% sucrose linear gradient, and sedimented by ultracentrifugation. Gradient fractions collected from the bottom, and each fraction was precipitated with anti-pp28 MAb and analyzed by SDS-PAGE. Note the presence of pp28 in fractions farther down the gradient in later chase intervals. (B) pp28 was transiently expressed in HK293 cells, and pp28 was fractionated in 5 to 40% sucrose gradient and analyzed as described above. The results shown as the percentage of total protein in each fraction. Note that with increasing chase interval ($T = 0$ versus 40 min) the pp28 migrated farther into the gradient, a finding consistent with increasing mass.

molecular-weight forms of pp28 argued against aggregation as an explanation of pp28 multimerization but did not rule out the possibility that pp28 associated with other cellular or viral proteins during the chase periods. This possibility was investigated by carrying out a similar experiment utilizing radiolabeling and pulse-chase analysis of pp28 that was transiently expressed in HK293 cells (Fig. 2B). After pulse-labeling and a 40-min chase interval, labeled proteins were fractionated as described above. The amount of precipitated protein was expressed as a percentage of the total pp28 in the gradient (Fig. 2B). In the absence of other viral functions, pp28 appeared to multimerize, as evidenced by its migration into the gradient with an increasing chase interval (Fig. 2B). These results indicated that pp28 multimerization was independent of other viral proteins but did not rule out the possibility that pp28 multimerization followed interaction with a cellular protein.

pp28 utilizes a single domain for self-interaction. To define sequences required for the multimerization of pp28, we performed pulldown assays. We generated a series of GST-pp28 fusion proteins in which GST was fused with full-length wild-type pp28 (GST-pp28WT); four truncated mutants expressing the first 33, 61, 90, and 123 aa of pp28 (GST-pp28Mut33, GST-pp28Mut61, GST-pp28Mut90, and GST-pp28Mut123, respectively); and three deletion mutants in which aa 26 to 33, aa 26 to 43, or the acidic domain of pp28 (aa 44 to 59) were deleted [GST–pp28Δ26-33, GST–pp28Δ26-43, and GST–pp28Δ44-59(ac), respectively], as detailed in Fig. 3A. This panel of GST-pp28 fusion proteins was expressed in *E. coli* and immobilized on glutathione beads. These immobilized GST-pp28 fusion proteins were then used to perform a pulldown of a soluble epitope-tagged full-length pp28 (BB-pp28), also expressed in *E. coli*. All GST-pp28 fusion proteins immobilized on beads were subjected to SDS-PAGE to normalize the input amounts of GST-pp28 fusion proteins in pulldown experiments (Fig. 3B). To verify the immunoreactivity of GST-pp28 fusion proteins immobilized on the beads, we performed immunoblots with a MAb specific for pp28 or antibody specifically reactive with the BB epitope. Except for the fusion proteins GST–pp28Δ26-33 and GST–pp28Δ26-43, all GST-pp28 fusion proteins were detected with the pp28-specific MAb but not with the BB epitope-specific MAb (Fig. 3B). Because the fusion proteins GST–pp28Δ26-33 and GST–pp28Δ26-43 were not reactive with the pp28 specific MAb, the epitope recognized by this MAb presumably included aa 26 to 33 of pp28. Under conditions producing equivalent concentrations of all GST-pp28 fusion proteins, the GST-pp28 fusion proteins were used to pull down a soluble BB-pp28 protein expressed in *E. coli*. After binding and washing, the beads were boiled, and the eluted proteins were subjected to SDS-PAGE and transferred to nitrocellulose membranes. Probing the membrane with an MAb specific for the BB epitope tag revealed that GST-pp28WT, as well each of the GST-pp28 mutants, but not GST alone, bound soluble BB-pp28 expressed from *E. coli* (Fig. 3C). When the quantity of the bound pp28 was analyzed by densitometry, the amounts of BB-pp28 bound on GST-pp28 mutants differed, indicating that specific domains contributed to wild-type level of pp28-pp28 interactions. The amounts of BB-pp28 bound on GST-pp28Mut33 and GST–pp28Δ26-43 were significantly less than that of GST-pp28WT and the other GST-pp28 mutants, including GST–pp28Δ26-33 (Fig. 3C). The result indicated that aa 34 to 43 contained amino acid sequences required for wild-type pp28-pp28 interactions and that the first 43 aa of pp28 contained a domain that was responsible for the self-interaction of pp28. In addition, GST-pp28Mut61

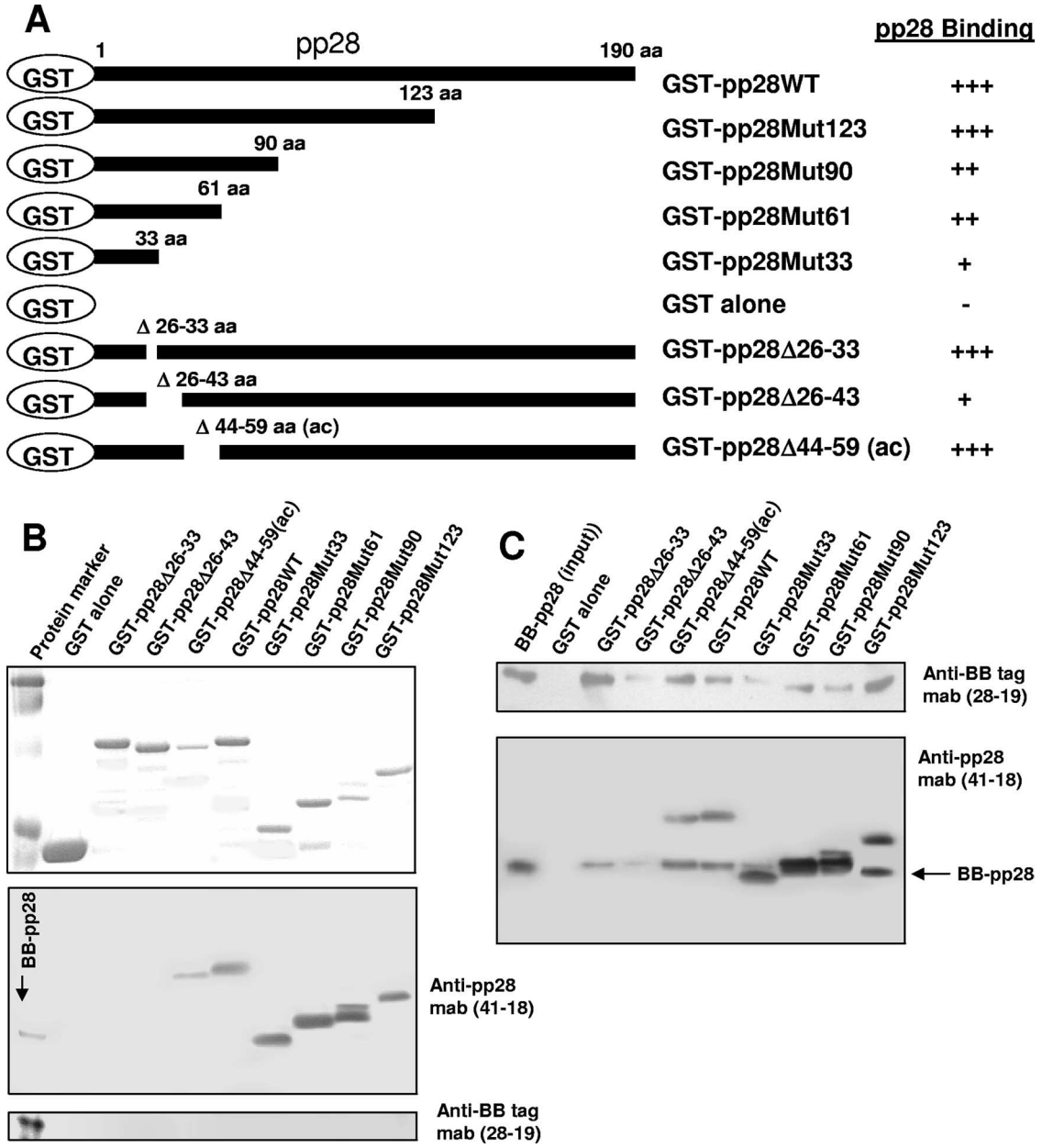

FIG. 3. Mapping of interacting domains of pp28 for the self-interaction by pulldown assays. (A) Schematic diagram of the GST-pp28 fusion proteins depicting the primary structure of the deletion mutants. Shaded horizontal bars indicate the residues expressed by the mutants. The pp28 binding activity of each mutant is presented at the right of the figure: +++, activity 100% of the wild type; ++, activity 70 to 90% of the wild type; +, activity <10% of the wild type; and −, activity 0% of the wild type. (B) SDS-PAGE analysis (top) showing the amounts of GST-pp28 fusion proteins on beads prior to pulldowns, and immunoblots (middle and bottom) showing antibody specificity of GST-pp28 fusion proteins on beads. Glutathione-conjugated beads with associated proteins were subjected to SDS-PAGE and visualized by Western blotting with anti-pp28 MAb and anti-BB tag MAb as described in Materials and Methods. Note that GST–pp28Δ26-33 and GST–pp28Δ26-43 were not detected by anti-pp28 MAb, indicating that the epitope recognized by this MAb included aa 26 to 33 of pp28. (C) Immunoblots showing the pp28 binding activity of deletion mutants. Equal amounts of the purified GST alone or GST-pp28 fusion proteins on beads in panel B were incubated with lysate from bacteria expressing BB tag-pp28. After extensive washing, bound proteins were subjected to SDS-PAGE and visualized by Western blotting with anti-pp28 MAb 41-18 and anti-BB tag MAb 28-19 as described above. The input lane shows 10% of the amount of the BB-pp28 fusion protein lysate that was added to the binding reaction.

and GST-pp28Mut90 exhibited a slight decrease in the binding of BB-pp28 compared to GST-pp28WT and GST-pp28Mut123, a mutant that binds with efficiency similar to that of wild-type pp28 (Fig. 3C). GST–pp28Δ44-59(ac) exhibited levels of binding similar to that of wild-type pp28, suggesting that the acidic amino acid cluster of pp28 did not have a direct role in pp28 multimerization, even though this region has a critical role in the intracellular trafficking of pp28 and production of infectious virus (Fig. 3C) (40). We also reprobed the membrane with an MAb specific for the pp28, and the same

patterns were observed, confirming the results from the pulldown assays (Fig. 3C). These results demonstrated that amino acid sequences within an amino-terminal domain of pp28 (i.e., aa 26 to 43) directed multimerization of this protein in absence of other viral and eukaryotic cellular proteins.

pp28-pp28 interactions occur at the ERGIC in transiently expressed cells. Studies from our laboratory have reported that pp28 is localized to the ERGIC in the absence of other viral proteins, and in results described above we demonstrated that pp28 multimerization did not require interactions with other viral proteins (37, 40). In the following experiments, we used FRET assays to investigate the cellular sites of pp28-pp28 interactions within mammalian cells and to further determine the sequence requirements for the intracellular self-interactions of pp28 in mammalian cells. Full-length pp28 and a panel of pp28 deletion mutants were fused with EGFP and coexpressed in Cos-7 cells, together with a full-length pp28 that was fused with monomeric red fluorescence protein (pp28-DsRed). FRET was then carried out utilizing a donor dequenching and acceptor photobleaching assay (Fig. 4). Importantly, this assay allowed us to detect pp28 interactions when pp28 and pp28 mutants were associated with the membranes of transfected cells. For FRET assays, EGFP fused with DsRed (EGFP-DsRed) was used as a positive control in transfected Cos-7 cells, and Golgi-associated, gamma adaptin ear-containing, ARF-binding protein 1 (GGA1) fused with EGFP (GGA1-EGFP) was used as a negative control. We selected a part of ERGIC as region of interest (ROI1) for FRET, and a nonbleaching region as an internal control (ROI2) after FRET (Fig. 4A). The FRET efficiency of a full-length pp28 or the first 61 aa of pp28 (pp28Mut61) (6 to 8%) was similar to that of the positive control EGFP-DsRed (7%), indicating that the first 61 aa, as well as full length, of pp28 could strongly interact with the full-length pp28 (pp28-DsRed; Fig. 4B). The result also showed that the pp28 self-interaction occurred in the ERGIC in the transfected cells, indicating that self-association of pp28 did not require additional viral functions, further confirming our results from GST-pulldown assays. The FRET efficiency of the deletion mutants containing the first 50, 35, and 30 aa of pp28 (~5%) was lower than that of pp28Mut61 (Fig. 4B), indicating that although the first 30 to 35 aa of pp28 was sufficient for interaction with the full length of pp28, the first 61 aa of pp28 appeared to be required for wild-type interactions. It is important to note that a recombinant virus expressing only aa 1 to 50 of pp28 is replication competent, albeit reduced in virus yield (41). In contrast, the FRET efficiency of a construct containing only the first 25 aa of pp28 (pp28Mut25) was zero (0%) (Fig. 4B), indicating no interaction with pp28-DsRed even though pp28Mut25 could be colocalized with full-length pp28 in the ERGIC by static immunofluorescence assays. Previous studies have documented the ERGIC localization of the pp28Mut25 mutant protein, suggesting that the ERGIC retention and/or localization signal of pp28 was distinct from the domain of this protein responsible for self-interactions (40). Somewhat different results were noted between FRET assays and GST-pulldown assays, suggesting that the pp28-pp28 interactions defined in these experiments were influenced by differences in expression systems, mammalian cells, and *E. coli*. Importantly, the GST-pp28 assays were performed in cell-free conditions in the presence of detergents, whereas the FRET assay utilized transfected cells that permitted membrane association of pp28 and the pp28 mutants, suggesting that self-association in the context of a membrane could be fundamentally different than that required for interactions between bacterially expressed proteins. Finally, it should be stressed that findings from both assays were consistent with the role of the amino terminus of pp28 in the multimerization of this protein.

pp28 multimerization is a postlocalization function of pp28 within the AC of cells infected with HCMV. Although the first 30 to 35 aa of pp28 have been reported to be sufficient for the localization of of pp28 to the ERGIC in transfected cells, the first 50 aa of pp28 was required for the localization of pp28 to the AC and for the assembly of infectious virus in infected cells (40). Furthermore, the first 61 aa of pp28 were required for the wild-type function of pp28 within the AC, as measured by the assembly and release of wild-type levels of infectious virus (40). To investigate the possible role of the multimerization of pp28 in the AC during virus assembly, we investigated the sequence requirement for pp28-pp28 interactions in different intracellular compartments of HCMV-infected cells by using FRET (Fig. 5). A DsRed-tagged full-length pp28 protein and pp28 mutant proteins tagged with EGFP were coexpressed in HFF cells after electroporation of plasmids encoding the first 61, 50, or 35 aa of pp28 (pp28Mut61-EGFP, pp28Mut50-EGFP, or pp28Mut35-EGFP). Electroporated HFF cells were then infected with HCMV 48 h later, and FRET assay was performed on the regions of interest, the AC (ROI1) and adjacent intracellular vesicles (ROI2 and ROI3) at 6 days postinfection (Fig. 5A). A significant level (>7%) of FRET was detected in the AC of cells expressing pp28Mut61, and a lower level (3 to 4%) was detected in the AC of cells expressing pp28Mut50 (Fig. 5B). This result was consistent with results that were obtained in cells transiently expressing pp28 and pp28 mutants (Fig. 4). However, the FRET efficiency of pp28Mut35 in the AC was significantly lower (<1%), suggesting that pp28Mut35 could multimerize in the ERGIC when transiently expressed in the absence of other viral proteins in transfected cells but failed to efficiently localize and to multimerize in the AC of virus-infected cells (Fig. 5B). This finding was consistent with our previous results that described the sequence requirements for the localization of pp28 to the AC and for the assembly of infectious virus (40). In addition, this result indicated that although the pp28Mut35 mutant formed multimers with full-length pp28 within the ERGIC of transfected cells as efficiently as the mutant pp28Mut50, it did not multimerize with wild-type pp28 in the ACs of infected cells. Thus, localization and accumulation of pp28 within the AC could be a prerequisite for multimerization of pp28. The FRET efficiency of pp28Mut61 or pp28Mut50 in the intracellular vesicles increased compared to that seen in the AC (6 to 8%), indicating that pp28 molecules in transiently expressed and/or infected cells interacted with each other in the adjacent intracellular vesicles, as well as in the AC (Fig. 5B). The FRET efficiency of pp28Mut35 in the intracellular vesicles was significantly less (<1%), although pp28Mut35 could be colocalized with full-length pp28 in the vesicles (Fig. 5B). Thus, it could be argued that the mutant pp28Mut35 lacked both an intact self-interacting domain and trafficking signals that efficiently localized this mutant to the AC and, therefore, multimer formation with wild-type pp28

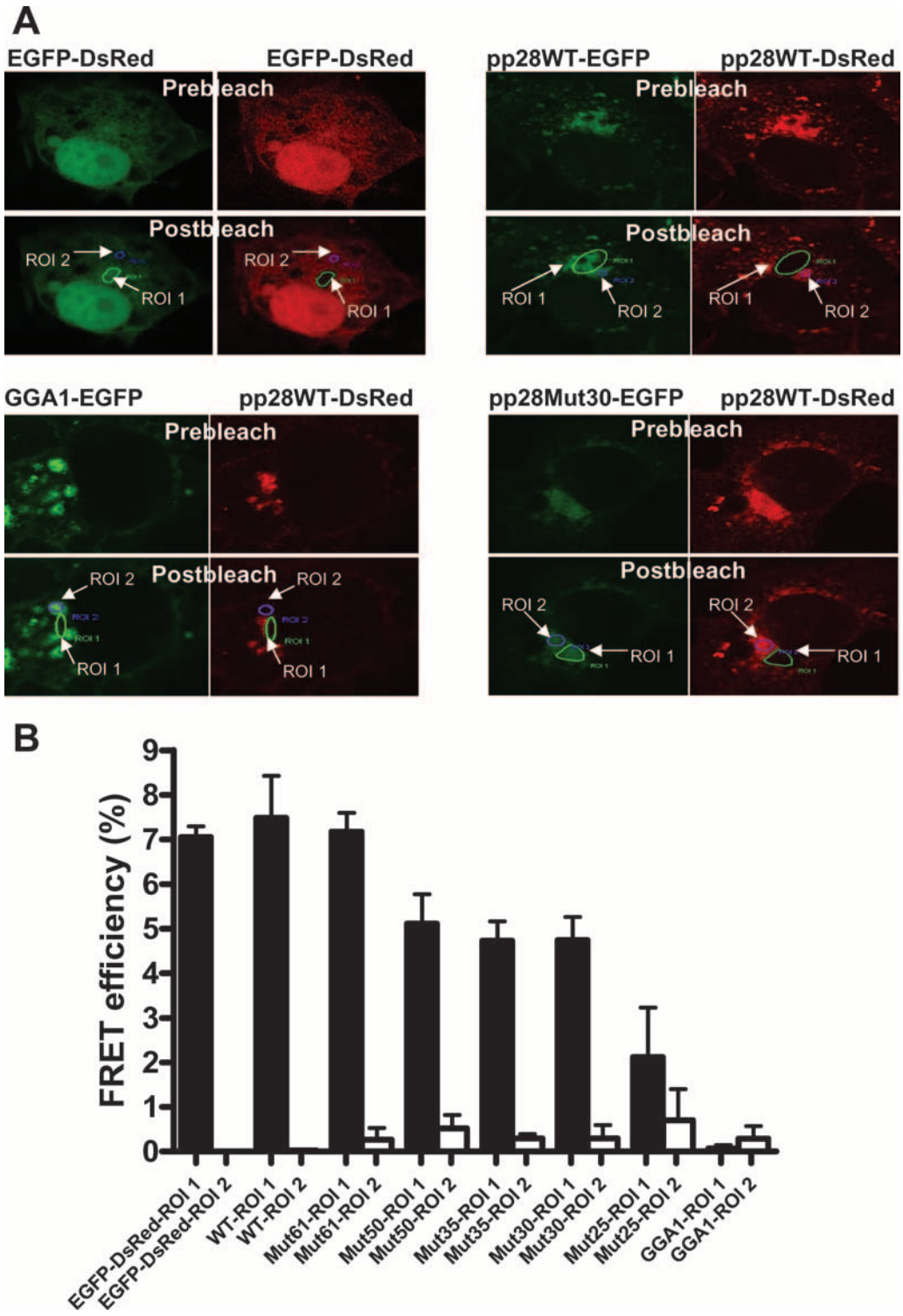

FIG. 4. FRET analysis of interactions of pp28 deletion mutants with the full-length pp28 protein within the ERGIC of transfected Cos-7 cells. (A) Pre- and postbleaching of cells expressing fusion proteins expressing EGFP and DsRed as a positive control. Cos-7 cells were cotransfected with approximately 3 μg of two expression plasmids encoding wild-type pp28-DsRed (pp28WT-DsRed) with wild-type pp28-EGFP (pp28WT-EGFP) or mutant pp28-EGFP (pp28Mut61-EGFP, pp28Mut50-EGFP, pp28Mut35-EGFP, pp28Mut30-EGFP, or pp28Mut25-EGFP). The cells were harvested at day 2 posttransfection, fixed with 2% paraformaldehyde, and analyzed by FRET assays as described in Materials and Methods. EGFP fused with DsRed (EGFP-DsRed) or Golgi-associated, gamma adaptin ear-containing, ARF-binding protein 1 (GGA1) fused with EGFP (GGA1-EGFP) were prepared as a positive or negative control in FRET assays, respectively. ROI indicates the region of interest (ERGIC). ROI 1, acceptor bleaching region; ROI 2, acceptor nonbleaching region as an internal (−) control. The enhancement in the intensity of EGFP after phtobleaching of dsRed signal is best illustrated by a signal increase in pp28WT-EGFP. (B) The efficiency of FRET was determined by using donor dequenching/acceptor photobleaching protocol (Leica, Nutley, NJ), and the FRET efficiency calculated as described in Materials and Methods. The FRET efficiency was statistically significant ($P < 0.001$) for all constructs except pp28Mut25 and GGA1 compared to the internal control. FRET from pp28Mut25 was significantly different from all other constructs ($P < 0.001$).

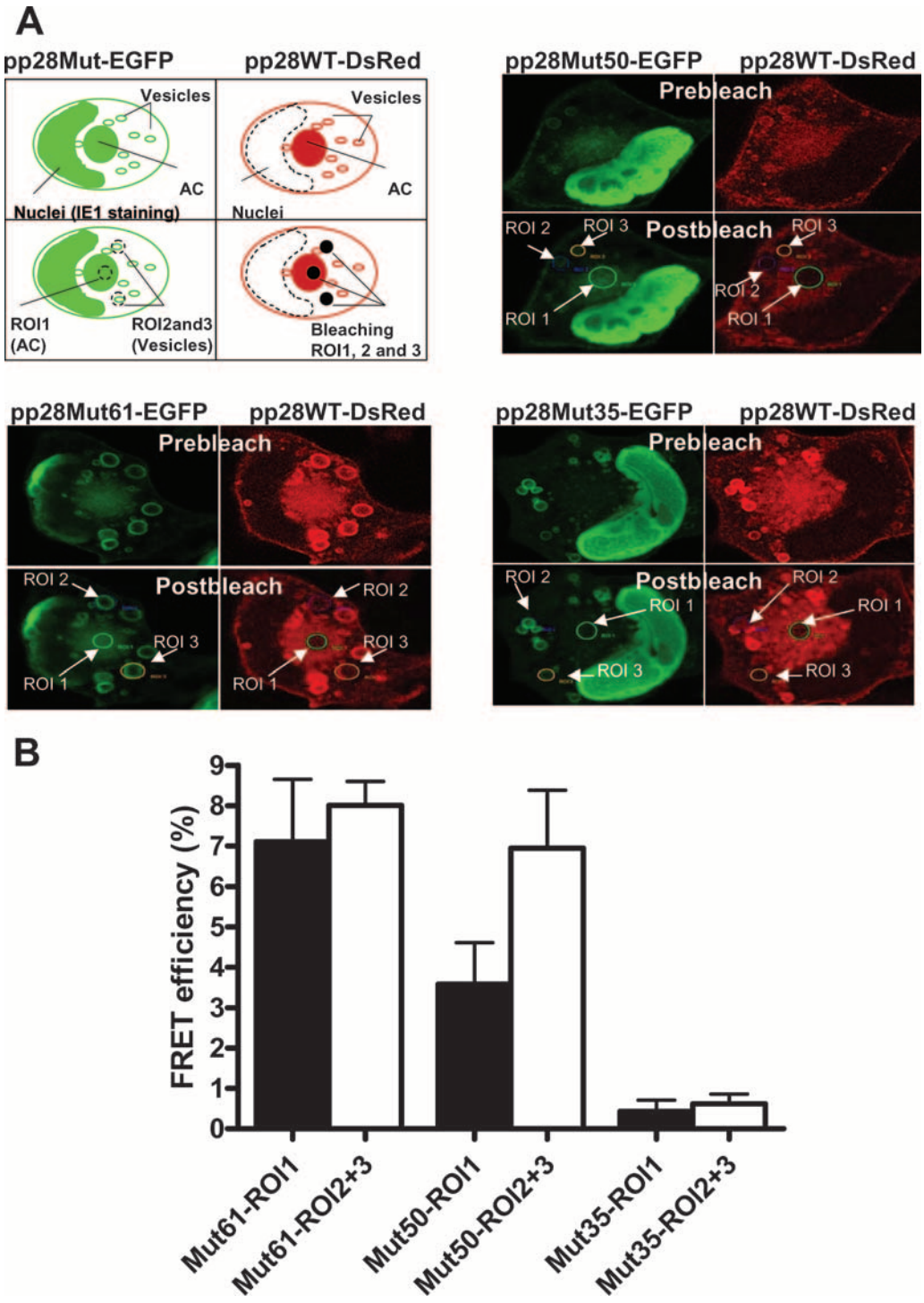

FIG. 5. FRET analysis of interactions of pp28 deletion mutants with the full-length pp28 protein within the AC and intracellular vesicles in HCMV-infected HFF cells. (A) Illustrations show the areas of FRET, a cell prior to bleaching (top) expressing EGFP (donor) and DsRed (acceptor), acceptor regions selectively bleached (bottom right, black dots), and donor regions measured in the intensity of EGFP postbleaching (bottom left, black circle). (B) Pre- and postbleaching of cells expressing EGFP and DsRed. HFF cells were electroporated with approximately 5 μg of two expression plasmids encoding wild-type pp28-DsRed (pp28WT-DsRed) with mutant pp28-EGFP (pp28Mut61-EGFP, pp28Mut50-EGFP, or pp28Mut35-EGFP) and infected 2 days later with HCMV at an MOI of 0.1. The cells were harvested at day 6 postinfection, fixed with 2% paraformaldehyde, stained with anti-IE-1 MAb followed by FITC-labeled anti-mouse IgG to identify infected cells (green nuclei), and analyzed by FRET assays. ROI indicates region of interest. ROI 1, AC; ROI 2 and 3, intracellular vesicles. (B) Efficiency of FRET determined as described above. The FRET efficiency in the AC and the intracellular vesicles was statistically significant ($P < 0.001$) for pp28Mut61 and pp28Mut50 compared to pp28Mut35. It was also noted that within the AC, FRET from pp28Mut61 was significantly different from pp28Mut50 ($P < 0.05$).

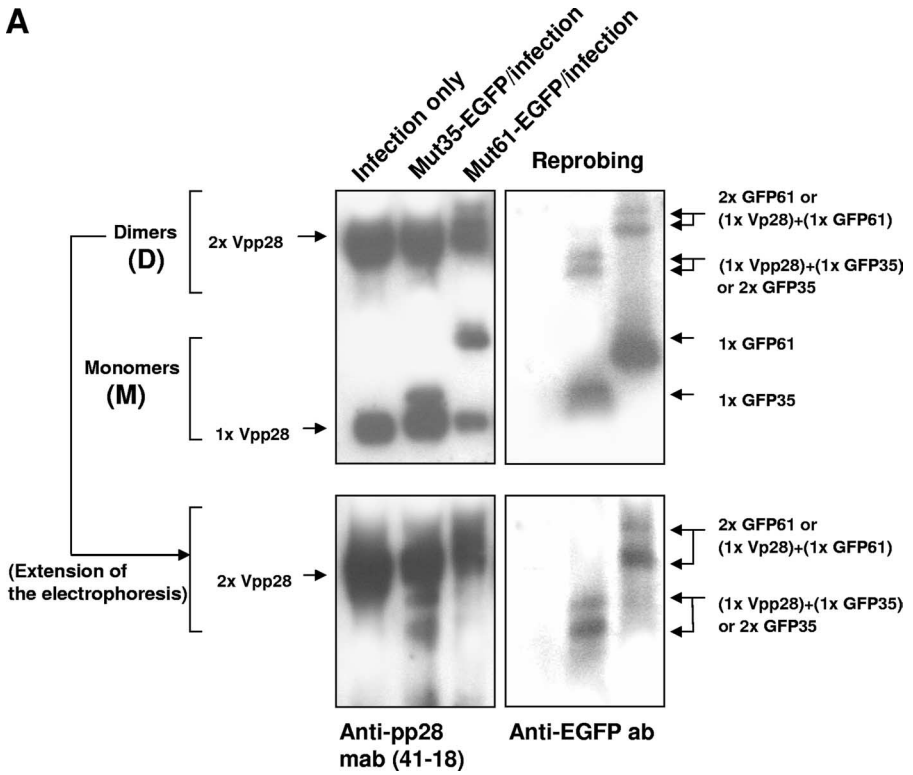

FIG. 6. Iodixanol density gradient fractionation of HCMV-infected HFF cells transfected with pp28 mutants. HFF cells were electroporated with approximately 5 μg of expression plasmids encoding pp28Mut61-EGFP or pp28Mut35-EGFP and infected 2 days later with HCMV at an MOI of 0.1. The cells were harvested at day 6 postinfection. (A) Expression of multimeric forms of pp28-EGFP fusion proteins and viral pp28. PNSs were prepared from the harvested cells, solubilized under lower concentrations of SDS (0.1% SDS) and nonreducing conditions, subjected to SDS-PAGE in 10% gel, and detected with anti-pp28 MAb and anti-EGFP polyclonal antibodies by immunoblotting. Note the faster migration of dimeric forms of pp28Mut35-EGFP compared to dimeric form of viral pp28, even though the predicted mass (in kilodaltons) from the amino acid sequence of pp28Mut35-EGFP is greater than that of viral pp28. PNS from cells infected with HCMV was prepared as a control. (B and C) Analysis of gradient fractions by immunoblotting. PNS were sedimented by centrifugation through iodixanol gradients as described in Materials and Methods. The gradient was fractionated by removing 1-ml fractions from the top. Thus, fraction 1 represents the top of the gradient, and fraction 10 represents the bottom of the gradient. Gradient fractions were analyzed by Western blotting. Proteins were detected with an antibody specific for pp28 or EGFP (top) as described in Materials and Methods and analyzed by densitometry (middle and bottom). The average density of the signal from protein in each gradient fraction was measured and plotted to provide graphic comparison of the pattern of fractionation of virus-encoded pp28 to those of pp28Mut61-EGFP (B) and pp28Mut35-EGFP (C) in monomeric forms (top) and in dimeric forms (bottom). Vpp28, GFP61, and GFP35 indicate viral pp28, pp28Mut61-EGFP, and pp28Mut35-EGFP, respectively. 1x and 2x indicate monomer and dimer, respectively. An asterisk (*) and two asterisks (**) indicate viral pp28 fractionated from HCMV-infected HFF cells that had been transfected with pp28Mut61-EGFP and pp28Mut35-EGFP, respectively. The membranes were stripped and reprobed with anti-CD63 MAb to identify gradient fractions containing endosomes (40).

was inefficient. These results, together with the results from FRET assays in transfected cells, argued that pp28 multimerization within the AC but not within other cellular compartments could be correlated with the assembly of infectious virions.

To further study the role of pp28 multimerization in virus assembly, we investigated the intracellular distribution of multimeric forms of pp28 late in infection in cells transfected with the mutants pp28Mut35-EGFP or pp28Mut61-EGFP and then infected with HCMV. We selected two molecules, pp28Mut35 and pp28Mut61, for this analysis for several reasons. In FRET assays, pp28Mut35 failed to accumulate and multimerize in the AC. In addition, it interacted weakly with wild-type pp28 within intracellular vesicles, suggesting that the pp28Mut35 failed to efficiently multimerize with wild-type viral pp28. Recombinant viruses constructed with pp28Mut35 failed to replicate. In contrast, the pp28Mut61 exhibited wild-type levels of accumulation in the AC, multimerized within the AC, and recombinant viruses constructed from this mutant replicated with wild-type virus kinetics. Therefore, these two mutant forms of pp28 allowed us to study the relationship between localization of pp28 to the AC and multimerization. PNSs were prepared from cells harvested late in infection (>6 days) and subjected to centrifugation through discontinuous iodixanol (Optiprep) density gradients, and individual fractions were analyzed by immunoblotting as described previously (Fig. 6). PNSs from cells transfected with pp28Mut35-EGFP or pp28Mut61-EGFP and then infected with HCMV were solubilized by using low concentrations of SDS (0.1%) and then analyzed in immunoblots. PNSs from HCMV-infected cells were used as a control. Monomeric and multimeric forms of pp28 molecules were detected by using a pp28 specific MAb and, after stripping of the same membrane, a polyclonal antibody specific for EGFP detected these same forms but not the forms that contained only wild-type virus encoded pp28 (Fig.

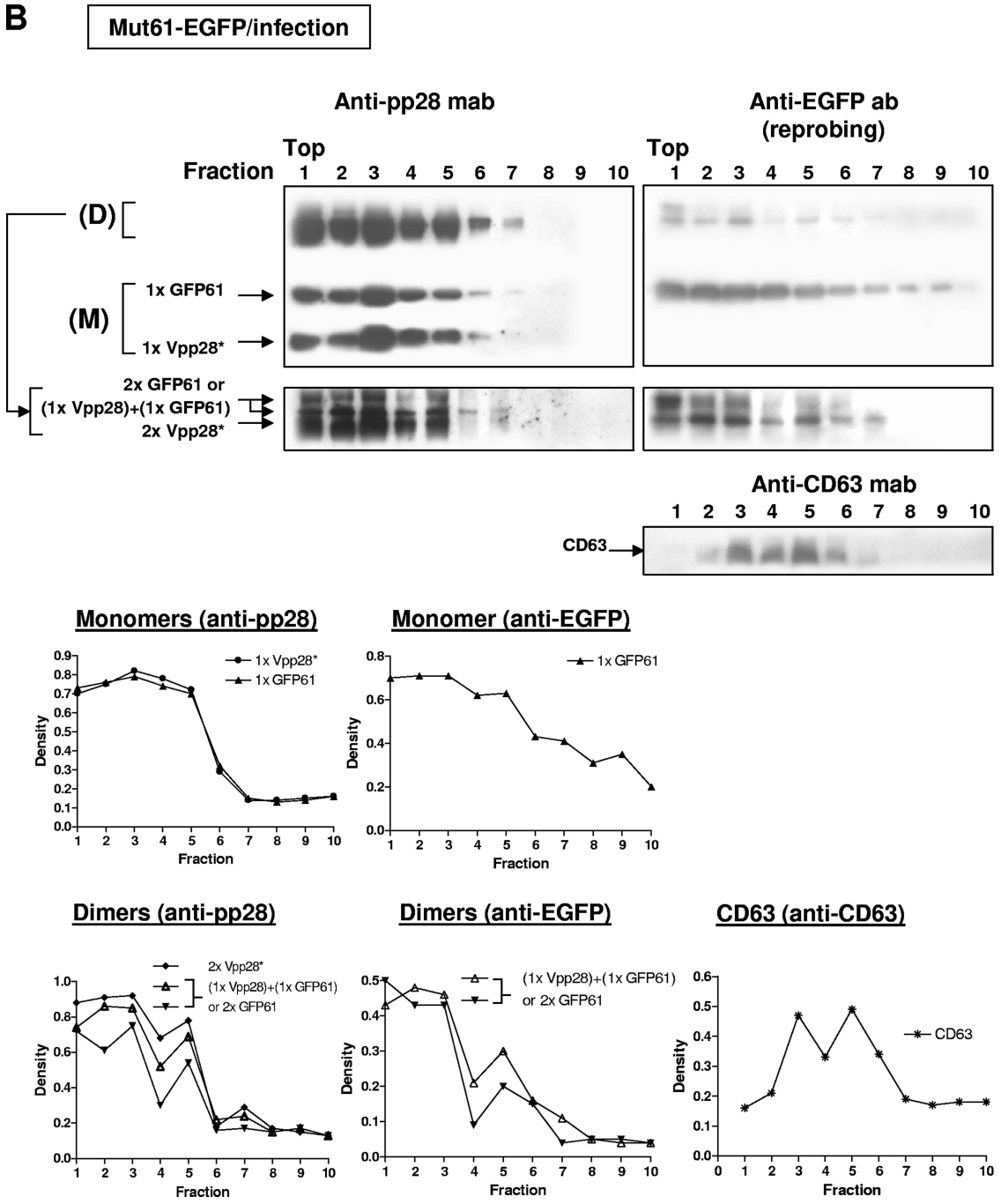

FIG. 6—*Continued*.

6A). As described previously, the pp28 molecules could be separated into monomer and dimers. According to the predicted molecular weights of pp28 molecules, the monomeric form of pp28Mut61-EGFP (1x GFP61) migrated more slowly than viral pp28 (1x Vpp28), and dimeric forms of pp28Mut61-EGFP (homodimer [2x GFP61] and heterodimer [1x GFP61 + 1x Vpp28]) migrated more slowly than similar forms of the viral pp28 (2x Vpp28). The monomeric form of pp28Mut35-EGFP (1x GFP35) migrated more slowly than viral pp28 (1x Vpp28), whereas the dimeric forms of pp28Mut35-EGFP (homodimer [2x GFP35] and heterodimer [1x GFP35 + 1× Vpp28]) migrated more rapidly than the corresponding forms of viral pp28 (2x Vpp28) (Fig. 6A). When we extended the duration of electrophoresis (allowing tracking dye to run off the gels) to resolve higher-molecular-weight forms, the differences in the migration of the various multimeric forms was more readily appreciated (Fig. 6A). A limitation of these experimental conditions was that we could not distinguish homodimers of pp28Mut61-EGFP (or pp28Mut35-EGFP) from a heterodimer of these molecules that contained viral pp28.

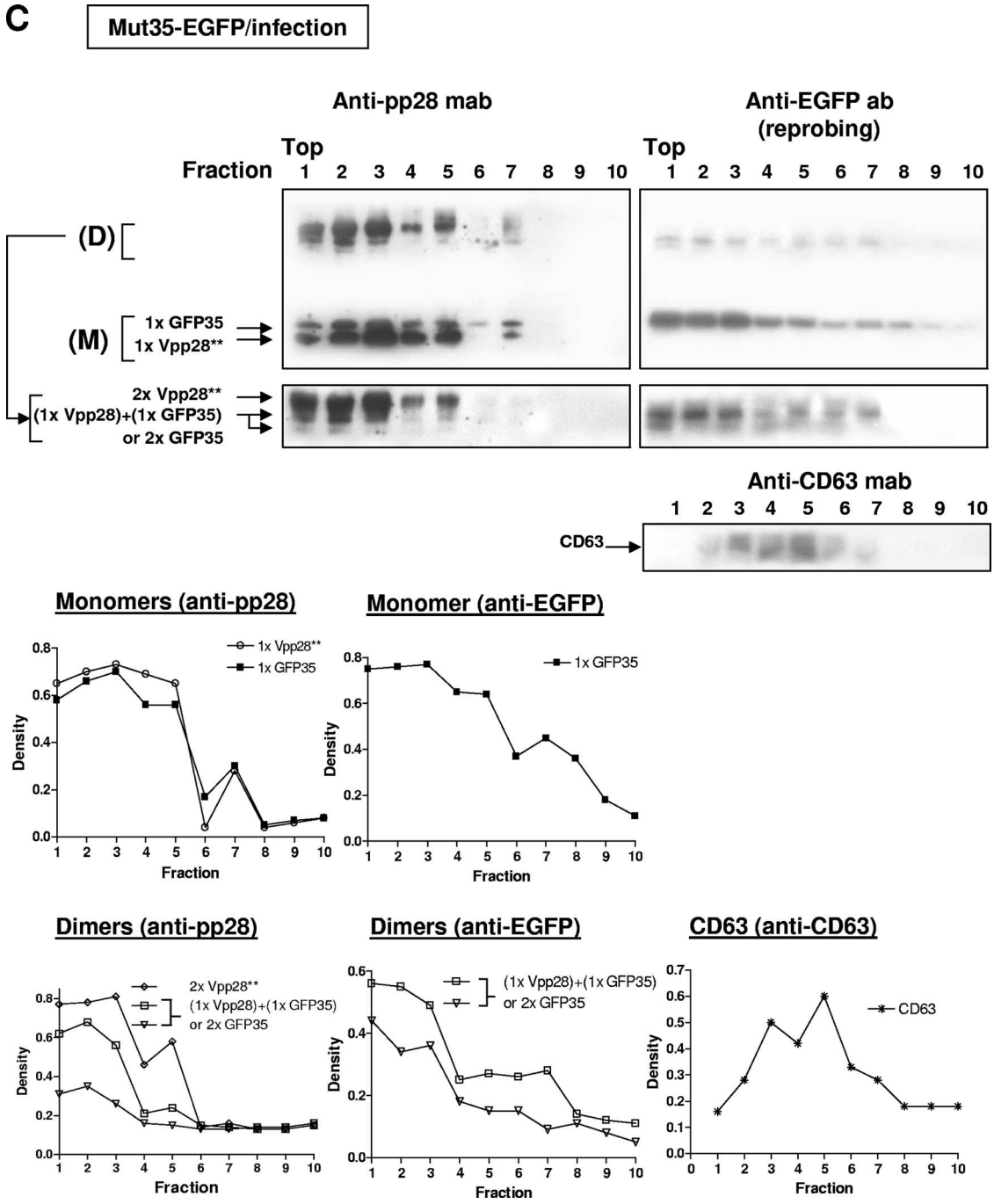

FIG. 6—*Continued*.

Based on the migrations of the different forms of molecules containing pp28, we analyzed individual fractions from density gradients by immunoblotting with antibodies specific for pp28 or EGFP (Fig. 6B and C). The intracellular distribution of pp28 was consistent with the distribution of the tetraspanin molecule CD63, a marker of late endosomal and/or lysosomal compartments that also localized within the AC (Fig. 6B) (25, 40). Using CD63 as a marker of the AC, analysis of gradient fractions revealed that the AC partitioned into two broad peaks, as we reported in a previous study (Fig. 6B) (40). The amount of protein detected in each fraction was then quantified by densitometry (Fig. 6B and C). The monomers of pp28Mut61-EGFP (1x GFP61) and viral pp28 (1x Vpp28) exhibited similar distributions within the gradient with the majority of these forms of pp28 migrating in the first three fractions of the gradient (Fig. 6B). The dimeric forms of these molecules exhibited a different pattern of distribution. Dimers of pp28Mut61-EGFP (2x GFP61 [or 1x GFP61 + 1× Vpp28]) or viral pp28 (2x Vpp28) were distributed in two peaks, with one broad peak being associated with the first three fractions

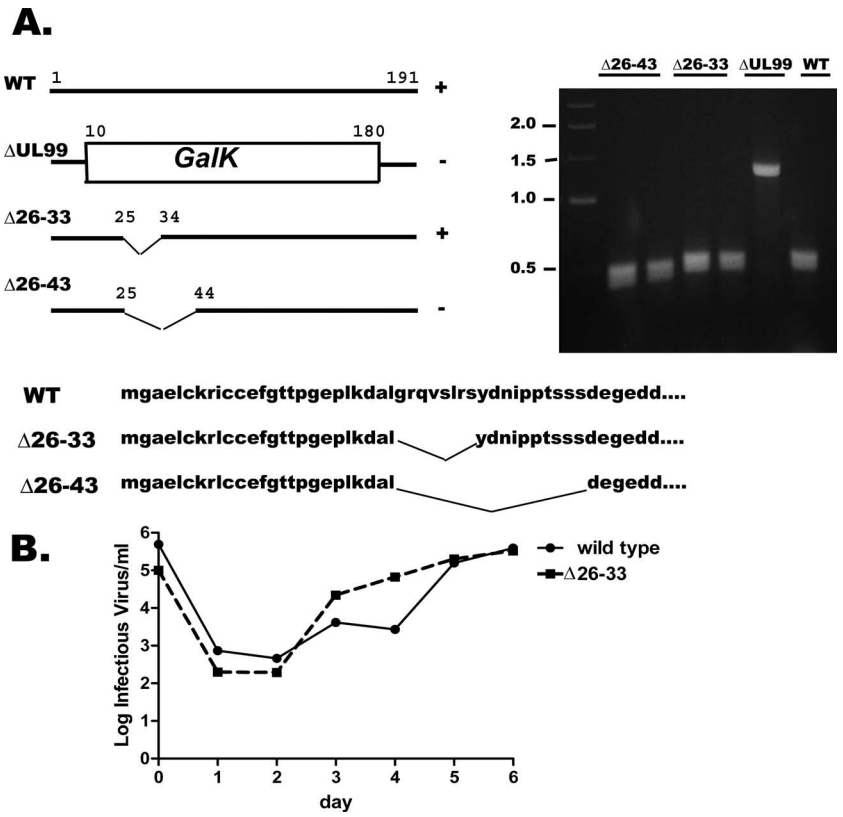

FIG. 7. Recovery of infectious HCMV following in-frame deletion of aa 26 to 33 but not aa 26 to 43 of pp28. (A) Diagram describing the recombinant HCMV BACs derived from wild-type HCMV BAC HB-5. Initially, UL99 deletion created by insertion of a *galK* cassette to create ΔUL99 BAC, this BAC was repaired with PCR products encoding the deletion/fusion UL99 ORFs, Δ26-33 and Δ26-43. Virus recovery after electroporation of BAC DNA was attempted in two separate experiments, and virus was recovered only from the wild type (WT) and the Δ26-33 mutant on both occasions (day 15 and day 21 postelectroporation) as indicated by the "+" symbol following the stick diagram. The agarose gel to the right demonstrates the size of the UL99 ORF when amplified by oligonucleotides designed to prime from the 5′ and 3′ ends of the ORF. Note the increase in size in the *galK* cassette containing ΔUL99 BAC and the decrease in size in two individual Δ26-43 BACs. The migration of the PCR product from two individual Δ26-33 BACs appears similar to the product from the wild-type BAC. The predicted amino acid sequence of the PCR products from the nucleotide sequence of the UL99 ORF of the recombinant BACs are shown with the in-frame deletions demarcated. (B) Virus yield curves from HFF cells infected with similar input amounts of WT and Δ26-33 viruses. Note that the growth curves are indistinguishable except for a single point (day 4).

and a second peak migrating further into the gradient (fraction 5; Fig. 6B). This result suggested that the sedimentation of dimeric forms of viral pp28 and pp28Mut61-EGFP differed from the corresponding monomeric forms of these proteins and was similar to the distribution of CD63 under these same gradient and sedimentation conditions (Fig. 6B) (40). The monomeric forms of pp28Mut35-EGFP (1x GFP35) exhibited a distribution in the gradient similar to that of the monomeric viral pp28, with the majority of this mutant pp28 protein migrating in the first three fractions of the gradient (Fig. 6C). In contrast to our finding with pp28Mut61, the dimeric forms of molecules containing the pp28Mut35 exhibited a different pattern of distribution. Two dimeric forms, a homodimer of pp28Mut35-EGFP (2x GFP35) and a heterodimer of viral pp28 and pp28Mut35-EGFP (1x GFP35 + 1x Vpp28) migrated in the first two to three fractions of the gradient, a distribution that was similar to that of monomeric forms of pp28 and pp28Mut61 (Fig. 6C). These results indicated that multimeric forms of pp28Mut61-EGFP and viral pp28 molecules cosedimented with the AC, whereas multimeric forms of the pp28Mut35 molecule sedimented with membranes containing components of the ER and Golgi that were found in the top of the gradient (Fig. 6C) (40). Together with our results from FRET assays, these findings suggested that pp28 multimerization associated with the assembly of infectious virions likely occurred after this protein was localized in the AC (postlocalization) and not in cellular compartments such as the ERGIC. Furthermore, these results suggested that the capacity of wild-type and mutant pp28 such as pp28Mut61 and pp28Mut50 to localize in the AC and to multimerize into higher-molecular-weight forms was required for the assembly of infectious virions.

The multimerization domain of pp28 (aa 34 to 43) is required for the assembly of infectious virions. To further investigate the role of multimerization in the assembly of infectious virus, we generated two recombinant HCMV-BACs by the deletion of aa 26 to 33 (Δ26-33) or aa 26 to 43 (Δ26-43) in the coding sequence of pp28 (UL99) (Fig. 7A). Amplification of this region of the BACs produced products of the expected size, and the sequences of these products indicated that the in-frame deletions were present in the recombinant BACs (Fig. 7A). HCMV-BACs containing these deletion mutants

were then electroporated into HFF cells. In two independent experiments, we successfully recovered replication-competent HCMV from the Δ26-33 BAC but not from the Δ26-43 BAC (Fig. 7). Virus was recovered from the control wild-type HCMV BAC DNA electroporated in each experiment, and the HCMV BAC containing a deletion of the entire ORF of UL99 (ΔUL99) failed to produce virus (Fig. 7A). Comparison of the growth curves between the recombinant virus mutΔ26-33 and wild-type HCMV revealed no differences in virus yield over a 6-day interval when HFF cells were infected with at an approximate MOI of 1 (Fig. 7B). Image analysis of the HFF cells electroporated with expression plasmids encoding EGFP-tagged pp28 mutΔ26-33 or mutΔ26-43 and then infected with wild-type HCMV revealed localization of the mutΔ26-33 within the AC but accumulation of mutΔ26-33 on the periphery of the AC within infected cells 6 days postinfection (data not shown). These results were reminiscent of previous findings that demonstrated that mutant forms of pp28 could traffic in and out of the AC and that only forms that supported virus replication accumulated in the AC (40, 41). Thus, it appeared that accumulation of pp28 within the AC required multimerization. Together, these results demonstrated the importance of aa 34 to 43 of pp28 in the assembly of HCMV and, together with the findings presented previously, argued that pp28 self-interactions leading to multimerization of this tegument protein were critical for virus assembly.

DISCUSSION

The importance of the multimerization of tegument proteins in the assembly of herpesviruses has not been well studied. In contrast, numerous reports in the literature have documented that the multimerization of matrix (tegument) proteins in structurally less complex RNA viruses play an essential role in virus assembly, particularly in the envelopment (budding) of the particle. As examples, the MAs in vesicular stomatitis virus, the paramyxovirus SV5, Ebola virus, influenza virus, Rous sarcoma virus, and human immunodeficiency virus type 1 (HIV-1) are membrane associated and are proposed to undergo multimerization to create lattice-like structures that have been proposed to lead to the eventual budding or pinching off of that region of the membrane (11, 13, 15, 16, 18, 20, 21, 27, 33, 35, 38, 39, 47, 54). Although the recruitment of host cellular functions is necessary for the budding of these viruses, multimerization of their MAs represents an essential viral function in this process (17, 19, 28, 33). In the present study, we have provided evidence consistent with the multimerization of the HCMV tegument protein, pp28, during the assembly of infectious particles. Mutant forms of pp28 that fail to efficiently multimerize within virus-infected cells do not support the production of infectious virus, suggesting that multimerization of pp28 was an essential step during the assembly of the infectious particle.

Previous studies from this and other laboratories have reported that additional higher-molecular-weight forms of pp28 could be observed in immunoblot analysis of pp28 from infected cells (22, 40). These higher-molecular-weight forms of pp28 were thought to represent either multimers of pp28 formed during assembly or, alternatively, misfolded forms of pp28 that aggregated into higher-molecular-weight species. In experiments presented here, we have provided evidence that the higher-molecular-weight forms were in fact multimers of pp28. Initially, we found that higher-molecular-weight forms of pp28 were readily detected under reduced concentrations of SDS (0.1% SDS) and nonreducing conditions of protein solubilization, raising the possibility that multimerization of pp28 could be mediated by intra- and interchain disulfide bonding. We also demonstrated the multimerization of pp28 in virus-infected cells by a pulse-chase analysis and sedimentation in sucrose gradients, indicating that multimers of pp28 exhibited kinetics during their formation, a finding that argued against the possibility that these higher-molecular-weight forms were simple aggregates of pp28. Pulse-chase analysis of transiently expressed pp28 molecule also indicated that pp28 could multimerize in absence of other viral proteins, presumably through self-interactions. Finally, multimer formation by bacterially expressed pp28 strongly argued that pp28 self-interactions were directed by the primary sequence of this tegument protein and not indirectly through other cellular or viral proteins.

The domains mediating pp28 multimerization were crudely mapped by using several independent techniques. Initially, we used a yeast two-hybrid screen to identify a large region consisting of the N-terminal third (the first 61 aa) of pp28 as a potential domain mediating pp28-pp28 interactions (data not shown). Experiments using GST pulldown assays of bacterially expressed protein suggested that pp28 multimer formation was dependent on the expression of aa 26 to 43 because the deletion of this sequence resulted in a significant decrease in interactions with the full length of pp28. This finding suggested that the first 43 aa of pp28 contained amino acid sequences that were essential for wild-type levels of self-interactions of pp28. The Δ26-33 deletion mutant interacted with pp28 at levels comparable to those of wild-type pp28, suggesting that within the essential first 43 aa of pp28, aa 34 to 43 played a critical role in pp28 self-interactions, at least as analyzed in GST-pulldown assays. Confirmation of this finding was provided by characterization of recombinant HCMV BACs; only the Δ26-33 BAC produced virus after electroporation into HFF cells (Fig. 7). The binding of other deletion mutants, including the Δ124-190 and Δ44-59(ac) mutants, was comparable to that of the full length of pp28, indicating that the C-terminal one-third of pp28, as well as the previously identified N-terminal acidic amino acid cluster, was not essential for wild-type pp28 self-interactions. Thus, even though the acidic amino acid cluster found between amino acids 44 to 59 of pp28 has an essential function in the trafficking and localization of pp28 in infected cells, as well as the production of infectious virus, this domain appeared to have no direct role in the multimerization of pp28 (40). Future studies will attempt to further define the role of individual amino acids within this 10-aa sequence that appears to be required for pp28 self-interactions. Finally, as noted above, other deletion mutants, such as the Δ62-190 or Δ91-190 pp28 deletion mutants, exhibited only minimal decreases in their interactions with the full length of pp28, providing additional evidence for the lack of any assignable functional role for the C-terminal aa 62 to 190 of pp28 in virion assembly (22, 40).

Using FRET, we attempted to identify the compartment within the infected cell in which pp28 multimerizes, a question directly relevant to the role of this tegument protein in the

cytoplasmic assembly of HCMV. We found that pp28-EGFP and pp28-DsRed proteins exhibited significant FRET within the ERGIC following their transient expression in the absence of other viral proteins. Furthermore, and in contrast to GST-pulldown assays, FRET assays of pp28 mutants transiently expressed in Cos-7 cells suggested that the first 30 to 35 aa of pp28 was sufficient for interaction with the full length of pp28, although the first 61 aa of pp28 appeared to be required for interactions that were similar to wild-type pp28. Previously, we have shown that localization of pp28 in the ERGIC required myristoylation at glycine 2 and, presumably, membrane association in this intracellular compartment (3, 40). These findings raised the possibility that pp28 multimerization could play a critical role in pp28-membrane binding or, alternatively, that membrane association was required for pp28 multimerization. Consistent with these possibilities have been findings in other viruses that have demonstrated a linkage between viral MA membrane association and multimerization (13, 14, 20, 35, 47). It has been reported that mutations in a 14-aa region between the capsid and nucleocapsid sequences in the Gag protein of HIV-1 inhibit Gag multimerization and, as a result, reduce membrane binding and that dimerization of the Rous sarcoma virus MA increased its capacity to associate with membrane in vitro (13, 20). In addition, structural studies of the HIV-1 MA have demonstrated that the multimerization leads to exposure of the myristate moiety (myristic acid switch) and membrane insertion of myristic acid, thereby presumably increasing the membrane binding of MA (47). FRET assays of pp28 mutants containing C-terminal deletions revealed that, in contrast to the first 30 to 35 aa of pp28, the first 25 aa of pp28 were not sufficient for interactions with the full length of pp28, although mutants containing only the first 25 aa colocalized with resident proteins of the ERGIC in transfected cells (40). In addition, previous findings from static immunofluorescence assays indicated that a pp28 mutant expressing the first 25 aa trafficked and localized within the ERGIC in transfected cells, whereas the nonmyristoylated pp28 mutant failed to colocalize with resident proteins of ERGIC (3, 40). Therefore, the binding or retention signal responsible for the localization of pp28 in the ERGIC that was expressed within the first 25 aa was distinct from the self-interacting domain of this protein. Together, these data suggested that multimerization of pp28 was not required for membrane association and, based on our findings with bacterially expressed forms of pp28, it could be argued that membrane association was not required for multimerization of this protein. However, it is important to consider that localization of pp28 within a membrane such as the ERGIC in transfected cells or in the AC in virus-infected cells could facilitate multimerization by fostering interaction of key domains of this protein or secondarily to increased local concentration of the protein. Such a possibility provided an explanation for the discrepant findings we observed in GST-pulldown assays and the FRET assay of transiently expressed pp28 mutants (see below).

When the results from FRET assays of transiently expressed pp28 mutants were compared to the results from the GST-pulldown assays, the minimal amino acid sequence required for pp28 self-interaction appeared to be different. Our results utilizing FRET suggested that only the first 30 aa of pp28 were required for self-interaction, whereas a bacterially expressed pp28 mutant containing only the NH_2-terminal 33 aa was significantly impaired in its capacity to bind wild-type pp28. Several possible differences between these assays could account for these different findings. The first is that the binding assay and the FRET are two very different assays and differ in their capacity to quantify differences in interactions between two molecules. The GST assay utilized in the present study was qualitative and provided an estimate of the relative binding interactions between mutant pp28 proteins and wild-type pp28. As an example, the GST-pulldown assay indicated that the binding of the pp28 deletion mutant, pp28Mut33 (aa 1 to 33), was significantly reduced compared to wild-type pp28, and yet detectable binding of the pp28Mut33 with pp28 was still observed. Such a level of binding could be sufficient to account for the positive findings from a more sensitive and quantitative assay that measured FRET between the pp28Mut33 and the wild-type protein. Second, pp28 expressed in mammalian cells undergoes posttranslational modifications, including phosphorylation, palmitoylation, and possibly ubiquitination (data not shown), that do not occur in *E. coli*. Thus, modifications within mammalian cells of specific residues within the interacting domains or even adjacent to interaction domains could potentially contribute to pp28-pp28 self-interactions when measured in FRET assays. Finally, as noted above, the concentrations of interacting proteins in FRET assays versus those in GST-pulldown assays were almost assuredly different, particularly the local concentrations of proteins. In transient-expression assays used for FRET analysis, individual proteins are overexpressed and concentrate within intracellular membranes, whereas GST-pulldown assays were done in solutions containing detergents and denatured proteins immobilized on Sepharose beads. Thus, the differences in the results obtained with GST-pulldown assays and FRET assays could be readily explained by differences both in the biochemical forms of the proteins assayed for interactions and in the sensitivity of these assays. Even with these limitations in mind, it is important to note that both assays were concordant in terms of identifying the amino terminus of pp28 (aa 1 to 43) as being required for efficient pp28 self-interactions. Admittedly, definition of the minimal sequence of pp28 within the first 43 aa that directs this self-interaction will require the generation and characterization of additional pp28 mutants, and yet our experiments have identified a previously unrecognized functional domain within the amino terminus of pp28 that was responsible for the multimerization of this tegument protein. Lastly, the precise role of this essential tegument protein in HCMV morphogenesis remains undefined, but the identification of a domain in the amino terminus of this protein responsible for the multimerization of pp28 suggested that this tegument protein may have a direct role in particle budding, perhaps one that is similar to that of other more well-studied viral MAs (11, 18, 21, 23, 39).

In contrast to findings from transient-expression assays, FRET assays of pp28 in transiently expressed and/or infected cells revealed that pp28-EGFP and pp28-DsRed proteins interacted with each other within the AC, as well as within adjacent intracellular vesicles. The derivation of these vesicles remains to be defined, but colocalization of virion structural protein, including both tegument and envelope proteins, within these vesicles suggested that they could be fragments of the membranous AC that were formed late in infection (36).

FRET analysis of C-terminal deletion pp28 mutants in transiently expressed and/or virus-infected HFF cells suggested that, as a minimal estimate, the first 50 aa of pp28 was required for the multimerization of pp28 within the AC. In addition, pp28Mut50 strongly interacted with the full length of pp28 in intracellular vesicles at levels that were comparable to the pp28Mut61 mutant protein. These findings raised the possibility that within the cytoplasmic vesicles, pp28Mut50 molecules were incorporated into pp28/pp28Mut50 multimers, whereas within the AC, interactions were considerably more dynamic and represented the average signal from forming and formed pp28/pp28Mut50 multimers. The interaction of pp28Mut50 with wild-type pp28 within the AC in infected cells was reduced compared to pp28Mut61, a finding consistent with the capacity of these different pp28 mutants when engineered into the viral genome to accumulate within the AC during virus assembly and to support virus assembly (41). These findings suggested that pp28 multimers formed with different efficiency within the AC depending on the presence of specific sequences in the pp28 deletion mutant. Consistent with this mechanism was the finding that although pp28Mut35 could multimerize in the ERGIC when overexpressed in transfected cells, it failed to accumulate in the AC and, as a result, failed to multimerize within the AC of the virus-infected cells. Thus, it could be proposed that the pp28Mut35 mutant failed to reach a sufficient concentration within membranes of the AC to foster a significant level of multimerization with wild-type pp28. This mechanism was consistent with our previous findings of the sequence requirements for localization of pp28 to the AC and assembly of infectious virus and therefore suggested that the accumulation of pp28 and mutant forms of pp28 within the AC was a prerequisite for multimerization (40, 41). Furthermore, in contrast to results from FRET analysis of pp28Mut50 and pp28Mut61, FRET assays of pp28Mut35 in intracellular vesicles, as well as in the AC of infected cells, provided no evidence supportive of pp28Mut35-pp28 interactions. The results suggested that in transient-expression and/or infection assays, mutant and wild-type pp28 molecules compete with wild-type viral pp28 for self-interaction in the intracellular vesicles, albeit at a different efficiency. Wild-type pp28 molecules interacted with pp28Mut50, pp28Mut61, or viral pp28 molecules with sufficient affinity to promote multimerization, whereas interactions with pp28Mut35 were much less efficient. Because pp28Mut35 was also defective in intracellular trafficking to the AC, it failed to accumulate at levels within the AC sufficient to promote interactions with pp28. Thus, there were at least two functional defects in the mutant pp28Mut35, a defect in efficient localization and a defect in self-interaction, that lead to defective multimerization of this mutant with wild-type pp28 in the AC. This mechanism was also supported by the finding that multimers of pp28Mut61 and pp28Mut50 but not pp28Mut35 partitioned in the AC based on their cosedimentation with wild-type pp28 in iodixanol gradient. Thus, multimerization of pp28 and of mutant forms of pp28 within the AC requires both efficient trafficking to this intracellular compartment and expression of an interaction domain with sufficient affinity to facilitate efficient self-interaction. It is also possible that multimerization itself could further shift the kinetics of accumulation of pp28 and pp28 mutants in the AC such that accumulation within the AC after multimerization is favored over exit from the AC. Our previous finding from fluorescence recovery after photobleaching assays with the mutant pp28Mut50 supported this interpretation and indicated that, at equilibrium, the trafficking of this mutant to the AC was similar to that of wild-type pp28 and pp28Mut61 but exit from the AC was at a faster rate than either wild-type pp28 and pp28Mut61 (41). If the rate of trafficking of the pp28Mut50 into the AC was only slightly delayed compared to wild-type pp28, then it could also be impaired in the rate of accumulation (concentration) and, therefore, in its multimerization. A decrease in multimerization would be associated with a greater rate of transit out of the AC and a decrease in the assembly of infectious virions, two previously reported observations in the studies of this mutant of pp28 (41). Our results utilizing plasmids encoding EGFP-tagged pp28 mutΔ28-33 and mutΔ28-33 in transfection and/or infection assays were consistent with this interpretation and demonstrated that accumulation of pp28 within the AC required self-interactions leading to multimerization.

Our results indicated that the requirements for pp28 multimerization in virus assembly were distinct from sequence requirements for pp28 trafficking. Furthermore, our findings have allowed us to exclude the possibility that pp28 multimerization in the ERGIC plays a role in the viral budding and, in contrast, argued that the multimerization in the AC played a critical role in the envelopment process and perhaps was directly linked to the budding of infectious virus. Using iodixanol gradients to fractionate subcellular compartments, we previously reported that the intracellular distribution of the AC containing the pp28 molecule was consistent with the distribution of the tetraspanin molecule CD63, a marker of the late endosomal or lysosomal compartment (40). In experiments presented here, the intracellular distributions of multimeric forms of wild-type viral pp28 and pp28 mutants expressing the first 61 aa (pp28Mut61) were consistent with previous findings of the distribution of pp28 in the AC under these gradient and sedimentation conditions, while the intracellular distribution of multimeric forms of pp28 mutants expressing the first 35 aa (pp28Mut35) did not cosediment with the AC. Together with previous findings that demonstrated that recombinant viruses encoding the pp28Mut61 protein but not the pp28Mut35 protein were replication competent, these results indicated that pp28 multimerization within the AC was required for viral assembly. Lastly, these findings, together with the FRET analysis of cells transfected with pp28Mut61 and pp28Mut35 and then infected with HCMV, argued that pp28 multimerization took place after localization of this tegument protein in the AC and represented an essential step in particle envelopment and the production of infectious virions.

ACKNOWLEDGMENTS

This study was supported by grants R01 AI35602 and R01 A150189 from the National Institutes of Health, National Institute of Allergy and Infectious Diseases.

REFERENCES

1. **Billstrom, M. A., and W. J. Britt.** 1995. Postoligomerization folding of human cytomegalovirus glycoprotein B: identification of folding intermediates and importance of disulfide bonding. J. Virol. **69:**7015–7022.
2. **Britt, W. J., M. A. Jarvis, D. D. Drummond, and M. Mach.** 2005. Antigenic domain 1 is required for oligomerization of human cytomegalovirus glycoprotein B. J. Virol. **79:**4066–4079.
3. **Britt, W., M. Jarvis, J.-Y. Seo, D. Drummond, and J. Nelson.** 2004. Rapid

genetic engineering of human cytomegalovirus using a lambda phage based linear recombination system: demonstration that pp28 (UL99) is essential for production of infectious virus. J. Virol. **78:**539–543.
4. **Britt, W. J., and C. A. Alford.** 1996. Cytomegalovirus, p. 2493–2523. *In* B. N. Fields, D. M. Knipe, and P. M. Howley (ed.), Fields virology, 3rd ed. Raven Press, New York, NY.
5. **Britt, W. J., and D. Auger.** 1986. Synthesis and processing of the envelope gp55-116 complex of human cytomegalovirus. J. Virol. **58:**185–191.
6. **Britt, W. J., and S. Boppana.** 2004. Human cytomegalovirus virion proteins. Hum. Immunol. **65:**395–402.
7. **Britt, W. J., M. A. Jarvis, D. D. Drummond, and M. Mach.** 2005. Antigenic domain 1 is required for oligomerization of human cytomegalovirus glycoprotein B. J. Virol. **79:**4066–4079.
8. **Britt, W. J., and L. G. Vugler.** 1992. Oligomerization of the human cytomegalovirus major envelope glycoprotein complex gB (gp55-116). J. Virol. **66:** 6747–6754.
9. **Burniston, M. T., A. Cimarelli, J. Colgan, S. P. Curtis, and J. Luban.** 1999. Human immunodeficiency virus type 1 Gag polyprotein multimerization requires the nucleocapsid domain and RNA and is promoted by the capsid-dimer interface and the basic region of matrix protein. J. Virol. **73:**8527–8540.
10. **Chee, M. S., A. T. Bankier, S. Beck, R. Bohni, C. M. Brown, R. Cerny, T. Horsnell, C. A. Hutchison, T. Kouzarides, J. A. Martignetti, E. Preddie, S. C. Satchwell, P. Tomlinson, K. M. Weston, and B. G. Barrell.** 1990. Analysis of the protein-coding content of the sequence of human cytomegalovirus strain AD169. Curr. Top. Microbiol. Immunol. **154:**125–170.
11. **Chong, L. D., and J. K. Rose.** 1993. Membrane association of functional vesicular stomatitis virus matrix protein in vivo. J. Virol. **67:**407–414.
12. **Cohen, G. H., V. J. Isola, J. Kuhns, P. W. Berman, and R. J. Eisenberg.** 1986. Localization of discontinuous epitopes of herpes simplex virus glycoprotein D: use of a nondenaturing ("native" gel) system of polyacrylamide gel electrophoresis coupled with Western blotting. J. Virol. **60:**157–166.
13. **Dalton, A. K., P. S. Murray, D. Murray, and V. M. Vogt.** 2005. Biochemical characterization of Rous sarcoma virus MA protein interaction with membranes. J. Virol. **79:**6227–6238.
14. **Demirov, D. G., and E. O. Freed.** 2004. Retrovirus budding. Virus Res. **106:**87–102.
15. **Fujiyoshi, Y., N. P. Kume, K. Sakata, and S. B. Sato.** 1994. Fine structure of influenza A virus observed by electron cryo-microscopy. EMBO J. **13:**318–326.
16. **Garoff, H., R. Hewson, and D. J. E. Opstelten.** 1998. Virus maturation by budding. Microbiol. Mol. Biol. Rev. **62:**1171–1190.
17. **Garrus, J. E., U. K. von Schwedler, O. W. Pornillos, S. G. Morham, K. H. Zavitz, H. E. Wang, D. A. Wettstein, K. M. Stray, M. Cote, R. L. Rich, D. G. Myszka, and W. I. Sundquist.** 2001. Tsg101 and the vacuolar protein sorting pathway are essential for HIV-1 budding. Cell **107:**55–65.
18. **Gaudin, Y., J. Sturgis, M. Doumith, A. Barge, B. Robert, and R. W. H. Ruigrok.** 1997. Conformational flexibility and polymerization of vesicular stomatitis virus matrix protein. J. Mol. Biol. **274:**816–825.
19. **Gottlinger, H. G.** 2001. The HIV-1 assembly machine. AIDS **15**(Suppl. 5)**:**S13–S20.
20. **Guo, X., A. Roldan, J. Hu, M. A. Wainberg, and C. Liang.** 2005. Mutation of the SP1 sequence impairs both multimerization and membrane-binding activities of human immunodeficiency virus type 1 Gag. J. Virol. **79:**1803–1812.
21. **Hill, C. P., D. Worthylake, D. P. Bancroft, A. M. Christensen, and W. I. Sundquist.** 1996. Crystal structures of the trimeric human immunodeficiency virus type 1 matrix protein: implications for membrane association and assembly. Proc. Natl. Acad. Sci. USA **93:**3099–3104.
22. **Jones, T. R., and S. W. Lee.** 2004. An acidic cluster of human cytomegalovirus UL99 tegument protein is required for trafficking and function. J. Virol. **78:**1488–1502.
23. **Justice, P. A., W. Sun, Y. Li, Z. Ye, P. R. Grigera, and R. R. Wagner.** 1995. Membrane vesiculation unction and exocytosis of wild-type and mutant matrix proteins of vesicular stomatitis virus. J. Virol. **69:**3156–3160.
24. **Kerry, J. A., M. A. Priddy, C. P. Kohler, T. L. Staley, D. Weber, T. R. Jones, and R. M. Stenberg.** 1997. Translational regulation of the human cytomegalovirus pp28 (UL99) late gene. J. Virol. **71:**981–987.
25. **Krzyzaniak, M., M. Mach, and W. J. Britt.** 2007. The cytoplasmic tail of glycoprotein M (gpUL100) expresses trafficking signals required for human cytomegalovirus assembly and replication. J. Virol. **81:**10316–10328.
26. **Luban, J., K. B. Alin, K. L. Bossolt, T. Humaran, and S. Goff.** 1992. Genetic assay for multimerization of retroviral gap polyproteins. J. Virol. **66:**5157–5160.
27. **Markwell, M. A. K., and C. F. Fox.** 1980. Protein-protein interactions within paramyxoviruses identified by native disulfide bonding or reversible chemical cross-linking. J. Virol. **33:**152–166.
28. **Martin-Serrano, J., T. Zang, and P. D. Bieniasz.** 2003. Role of ESCRT-I in retroviral budding. J. Virol. **77:**4794–4804.
29. **Mettenleiter, T. C.** 2002. Herpesvirus assembly and egress. J. Virol. **76:**1537–1547.
30. **Meyer, H., A. Bankier, M. P. Landini, and R. Ruger.** 1988. Identification and procaryotic expression of the gene coding for the highly immunogenic 28-kilodalton structural phosphoprotein (pp28) of human cytomegalovirus. J. Virol. **62:**2243–2250.
31. **Mocarski, E. S., and C. Tan Courcelle.** 2001. Cytomegaloviruses and their replication, p. 2629–2673. *In* D. M. Knipe and P. M. Howley (ed.), Fields virology, 4th ed., vol. 2. Lippincott/Williams & Wilkins, Philadelphia, PA.
32. **Murphy, E., D. Yu, J. Grimwood, J. Schmutz, M. Dickson, M. A. Jarvis, G. Hahn, J. A. Nelson, R. M. Myers, and T. E. Shenk.** 2003. Coding potential of laboratory and clinical strains of human cytomegalovirus. Proc. Natl. Acad. Sci. USA **100:**14976–14981.
33. **Pornillos, O., J. E. Garrus, and W. I. Sundquist.** 2002. Mechanisms of enveloped RNA virus budding. Trends Cell Biol. **12:**569–579.
34. **Rubin, R.** 2002. Clinical approach to infection in the compromised host, p. 573–679. *In* R. Rubin and L. S. Young (ed.), Infection in the organ transplant recipient. Kluwer Academic Press, Inc., New York, NY.
35. **Saad, J. S., J. Miller, J. Tai, A. Kim, R. H. Ghanam, and M. F. Summers.** 2006. Structural basis for targeting HIV-1 Gag proteins to the plasma membrane for virus assembly. Proc. Natl. Acad. Sci. USA **103:**11364–11369.
36. **Sanchez, V., K. D. Greis, E. Sztul, and W. J. Britt.** 2000. Accumulation of virion tegument and envelope proteins in a stable cytoplasmic compartment during human cytomegalovirus replication: characterization of a potential site of virus assembly. J. Virol. **74:**975–986.
37. **Sanchez, V., E. Sztul, and W. J. Britt.** 2000. Human cytomegalovirus pp28 (UL99) localizes to a cytoplasmic compartment which overlaps the endoplasmic reticulum-Golgi-intermediate compartment. J. Virol. **74:**3842–3851.
38. **Schnell, M. J., L. Buonocore, E. Boritz, H. P. Ghosh, R. Chernish, and J. K. Rose.** 1998. Requirement for a nonspecific glycoprotein cytoplasmic domain sequence to drive efficient budding of vesicular stomatitis virus. EMBO J. **17:**1289–1296.
39. **Scianimanico, S., G. Schoehn, J. Timmins, R. H. Ruigrok, H. D. Klenk, and W. Weissenhorn.** 2000. Membrane association induces a conformational change in the Ebola virus matrix protein. EMBO J. **19:**6732–6741.
40. **Seo, J., and W. Britt.** 2006. Sequence requirements for localization of human cytomegalovirus tegument protein pp28 to the virus assembly compartment and for assembly of infectious virus. J. Virol. **80:**5611–5626.
41. **Seo, J. Y., and W. J. Britt.** 2007. Cytoplasmic envelopment of human cytomegalovirus requires the postlocalization function of tegument protein pp28 within the assembly compartment. J. Virol. **81:**6536–6547.
42. **Silva, M. C., Q. C. Yu, L. Enquist, and T. Shenk.** 2003. Human cytomegalovirus UL99-encoded pp28 is required for the cytoplasmic envelopment of tegument-associated capsids. J. Virol. **77:**10594–10605.
43. **Sims, A. C., J. Ostermann, and M. R. Denison.** 2000. Mouse hepatitis virus replicase proteins associate with two distinct populations of intracellular membranes. J. Virol. **74:**5647–5654.
44. **Smith, J. D., and E. DeHarven.** 1973. Herpes simplex virus and human cytomegalovirus replication in WI-38 cells. I. Sequence of viral replication. J. Virol. **12:**919–930.
45. **Stagno, S., and W. J. Britt.** 2006. Cytomegalovirus. *In* J. S. Remington and J. O. Klein (ed.), Infectious diseases of the fetus and newborn infant, 6th ed. Elsevier Saunders, Philadelphia, PA.
46. **Streblow, D. N., S. L. Orloff, and J. A. Nelson.** 2001. Do pathogens accelerate atherosclerosis? J. Nutr. **131:**2798S–2804S.
47. **Tang, C., E. Loeliger, P. Luncsford, I. Kinde, D. Beckett, and M. F. Summers.** 2004. Entropic switch regulates myristate exposure in the HIV-1 matrix protein. Proc. Natl. Acad. Sci. USA **101:**517–522.
48. **Tooze, J., M. Hollinshead, B. Reis, K. Radsak, and H. Kern.** 1993. Progeny vaccinia and human cytomegalovirus particles utilize early endosomal cisternae for their envelopes. Eur. J. Cell Biol. **601:**163–178.
49. **Trus, B. L., W. Gibson, N. Cheng, and A. C. Steven.** 1999. Capsid structure of simian cytomegalovirus from cryoelectron microscopy: evidence for tegument attachment sites. J. Virol. **73:**2181–2192. (Erratum, **73:**4530.)
50. **Varnum, S. M., D. N. Streblow, M. E. Monroe, P. Smith, K. J. Auberry, L. Pasa-Tolic, D. Wang, D. G. Camp, K. Rodland, S. Wiley, W. Britt, T. Shenk, R. D. Smith, and J. A. Nelson.** 2004. Identification of proteins in human cytomegalovirus (HCMV) particles: the HCMV proteome. J. Virol. **78:**10960–10966.
51. **Warming, S., N. Costantino, D. L. Court, N. A. Jenkins, and N. G. Copeland.** 2005. Simple and highly efficient BAC recombineering using *galK* selection. Nucleic Acids Res. **33:**e36.
52. **Wentz-Hunter, K., R. Kubota, X. Shen, and B. Y. Yue.** 2004. Extracellular myocilin affects activity of human trabecular meshwork cells. J. Cell. Physiol. **200:**45–52.
53. **Yu, X., S. Shah, I. Atanasov, P. Lo, F. Liu, W. J. Britt, and Z. H. Zhou.** 2005. Three-dimensional localization of the smallest capsid protein in the human cytomegalovirus capsid. J. Virol. **79:**1327–1332.
54. **Zhao, H., M. Ekstrom, and H. Garoff.** 1998. The M1 and NP proteins of influenza A virus form homo- but not heterooligomeric complexes when coexpressed in BHK-21 cells. J. Gen. Virol. **79:**2435–2446.
55. **Zhou, Z. H., M. Dougherty, J. Jakana, J. He, F. J. Rixon, and W. Chiu.** 2000. Seeing the herpesvirus capsid at 8.5 Å. Science **288:**877–880.